Long-term stabilization of deep soil carbon by fire and burial during early Holocene climate change

Erika Marin-Spiotta[1,2]*, Nina T. Chaopricha[2], Alain F. Plante[3], Aaron F. Diefendorf[4], Carsten W. Mueller[5], A. Stuart Grandy[6] and Joseph A. Mason[1]

Buried soils contain large reservoirs of organic carbon at depths that are not typically included in regional and global soil carbon inventories[1]. One such palaeosol, the Brady soil of southwestern Nebraska, USA, is buried under six metres of loess. The Brady soil developed at the land surface on the late-Pleistocene-aged Peoria Loess in a period of warmth and wetness during which dunefields and dust sources across the region were stabilized[2,3]. Abrupt climate change in the early Holocene led to increased loess deposition that buried the soil[4]. Here, we used spectroscopic and isotopic analyses to determine the composition and stability of organic carbon in the Brady soil. We identify high levels of black carbon, indicating extensive biomass burning. In addition, we found intact vascular plant lipids in soil organic matter with radiocarbon ages ranging from 10,500 to 12,400 cal yr BP, indicating decomposition was slowed by rapid burial at the start of the Holocene. We conclude that landscape disturbance caused by abrupt climate change, fire and the loss of vegetative cover contributed to deep carbon sequestration as the soil was quickly buried under accumulating loess. We suggest that terrestrial soil carbon storage in arid and semi-arid environments could undergo landscape-scale shifts in response to rising temperatures, increased fire activity or drought.

Recent recognition that deep soil carbon (C) pools can respond on annual timescales to environmental change at the land surface has focused attention on understanding the source, composition and reactivity of organic carbon (OC) in deep soils[5–7]. Few studies have considered the role of soil erosion in the delivery, accumulation and persistence of soil C at depth. Soil erosion can regulate sinks and sources of atmospheric C through the deposition of organic matter in sites less favourable for decomposition and through the mobilization and oxidation of terrestrial C during transport[8,9]. Landscape disturbance and erosion driven by changes in climate, human activities or episodic events such as landslides and floods can also sequester C below ground by the burial of surface soils[1,10]. Whereas deep soil layers are commonly characterized by low OC concentrations, burial of former surface soil can lead to the persistence of large amounts of OC in deep soils that have become isolated from surface conditions. The accumulation of thick (>1 m) or impervious overlying sediments can contribute to long C residence times in buried soils by decreasing or preventing microbial decomposition through the slow recharge of oxygen and moisture and the depletion of nutrient-rich and energetically favourable substrates[1,11].

Wildfires can promote OC burial through the removal of vegetative cover and the facilitation of soil erosion by wind or water[12]. Fire also contributes to soil organic matter (SOM) persistence through thermal transformations into highly condensed aromatic compounds formed during incomplete combustion, known as black carbon (BC). BC may persist for hundreds to thousands of years in buried soils where microbial activity is limited by the scarcity of labile substrates, nutrients, moisture or oxygen, and where the dominance of organo-mineral interactions facilitates C protection from decomposers and their enzymes[7]. Addressing interactions between fire and erosion will improve estimates of terrestrial C sequestration and feedbacks to climate.

Here, we report on the role of fire and burial by dust aggradation in the accumulation and persistence of OC in a deeply buried palaeosol. Located in loess-mantled uplands at depths of 6–7 m, the Brady soil is characterized by a dark-coloured A horizon up to 1 m in thickness with large OC concentrations compared to the other soil layers in the loess-palaeosol sequence[3]. Identification of the Brady soil at multiple locations across the Central Great Plains suggests its formation was representative of regional environmental change at the time (Fig. 1; refs 2,13). Radiocarbon ages for the Brady SOM (Table 1) correspond with the time of active soil formation during the Pleistocene–Holocene transition and are well-constrained by optically stimulated luminescence (OSL) and radiocarbon dating of overlying and underlying loess[14]. Before the formation of the Brady soil, rates of local loess accumulation during the Pleistocene have been estimated at a remarkable 4 m kyr^{-1} (refs 3,13,14). Formation of the Brady soil initiated between 15,500 and 13,500 cal yr BP, during a time period of much slower dust deposition (0.1–0.2 m kyr^{-1}), which allowed for pedogenesis and the accumulation of SOM (refs 3,13,14). Increasing rates of loess deposition over time, estimated at 0.72–0.80 m kyr^{-1}, buried the Brady soil approximately 10,500–9,000 years ago[14].

Thermal and chemical analyses revealed large differences in the composition and stability of SOM in the Brady soil compared to the modern surface soil. The buried SOM had much greater thermal stability than the modern topsoil SOM, requiring greater combustion temperatures to reach 50% mass loss and CO_2 evolution (Table 1). This thermal stability indicates that the buried SOM is composed of compounds that require greater amounts of energy to

[1]Department of Geography, University of Wisconsin-Madison, Madison, Wisconsin 53706, USA, [2]Nelson Institute for Environmental Studies, University of Wisconsin-Madison, Madison, Wisconsin 53706 , USA, [3]Department of Earth and Environmental Science, University of Pennsylvania, Philadelphia, Pennsylvania 19104, USA, [4]Department of Geology, University of Cincinnati, Cincinnati, Ohio 45221, USA, [5]Lehrstuhl für Bodenkunde, Department of Ecology and Ecosystem Management, Center of Life and Food Sciences Weihenstephan, Technische Universität München, D-85350, Freisling-Weihenstephan, Germany, [6]Department of Natural Resources and the Environment, University of New Hampshire, Durham, New Hampshire 03824, USA. *e-mail: marinspiotta@wisc.edu
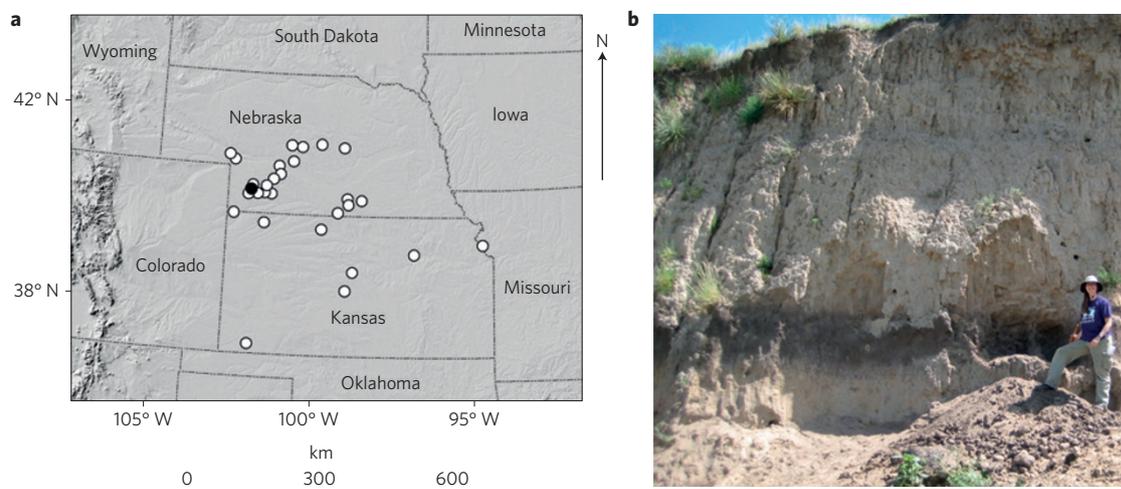
Figure 1 | The Brady soil palaeosol developed on late-Pleistocene Peoria Loess and was buried by aggrading loess in the early Holocene. a, Location of the Wauneta site (black dot) in southwestern Nebraska, USA, where samples were collected for this study, and locations of other sites (white dots) in the surrounding Central Great Plains region where discrete occurrences of the Brady soil have been identified[2,13]. **b**, Photo from the New Wauneta Roadcut in southwestern Nebraska showing the dark Brady soil at 6 m depth in loess.

Table 1 | Properties of bulk soils and fine (<20 μm) occluded particulate organic matter (oPOM-small) sampled from modern surface soil A horizons and buried Brady soil A horizons in Holocene-aged loess deposits in southwestern Nebraska, USA.

Soil fraction	Bulk soil		oPOM-small	
Soil layer	Modern soil	Brady soil	Modern soil	Brady soil
Depth (m)	0–0.12	6.35–6.5	0–0.12	6.35–6.5
Munsell color	10YR 3/2 (very dark greyish brown) to 10YR 3/3 (dark brown)	10YR 3/2 (very dark greyish brown) to 10YR 4/3 (brown)	10YR 2/2 very dark brown	10YR 2/1 black
SOC (%)	0.97 ± 0.27	0.62 ± 0.05	18.37 ± 0.37	14.34 ± 2.13
Molar C:N	8.24 ± 0.87	7.97 ± 0.71	12.86 ± 0.45	20.89 ± 0.65
SOC $\delta^{13}C$ (%)	-20.05 ± 2.22	-17.24 ± 0.41	-21.09 ± 3.02	-18.28 ± 0.05
SOC Fraction Modern	1.022 ± 0.046	0.288 ± 0.010	1.085 ± 0.040	0.288 ± 0.003
SOC $\Delta^{14}C$	14.2 ± 46.0	-714.8 ± 10.0	77.3 ± 40.0	-714.0 ± 3.0
SOC ^{14}C-age (cal yr BP) ranges (low to high)	Modern	$11,300 \pm 380$ to $12,010 \pm 410$	Modern to 180	$11,350 \pm 60$ to $11,690 \pm 120$
TG-T_{50} (°C)*	392 ± 4	433 ± 1	366 ± 3	412 ± 5
CO_2-T_{50} (°C)†	391 ± 3	432 ± 3	411 ± 2	444 ± 7
Energy density (J mg^{-1}C)‡	16.1 ± 2.1	13.1 ± 3.3	27.4 ± 1.4	36.9 ± 4.2
Aromatic C (%)§	$18.19 \pm 0.97^{\parallel}$	$43.16 \pm 0.88^{\parallel}$	17.49 ± 0.14	65.37 ± 0.08
Black C (%)¶	$11.0^{\parallel}$	$43.8^{\parallel}$	3.9	71.8
Lignin (%)¶	$0^{\parallel}$	$0^{\parallel}$	18.7	0
Lipid (%)¶	$10.1^{\parallel}$	$8.1^{\parallel}$	28.1	8.1
Lignin (%)#	9.3 ± 7.1	1.9 ± 1.2	6.6 ± 3.3	0.1 ± 0.07
Lipid (%)#	9.1 ± 0.9	20.8 ± 4.8	16.8 ± 2.2	28.8 ± 1.5
Polysaccharides (%)#	11.6 ± 1.0	4.9 ± 0.02	14.0 ± 0.4	5.6 ± 1.1
Total extractable lipids (mg g^{-1} C)**	15.3 ± 6.6	3.3 ± 2.1	4.0	6.1 ± 0.6
Bacterial/vascular plant leaf wax ratio++	0.24 ± 0.11	0.19 ± 0.02	0.38	0.75 ± 0.25

*The temperature at which 50% of sample mass is lost during thermogravimetric (TG) analysis. Mean ± 1 s.d. †The temperature at which 50% of sample OM is evolved as CO_2 during ramped combustion thermal analysis. Mean ± 1 s.d. ‡Determined as the area under the exothermic region (150–615 °C) of the differential scanning calorimetry (DSC) thermogram, normalized by the initial sample C mass. Mean ± 1 s.d. §Proportion of total spectral signal intensity in the 110–160 ppm region determined by ^{13}C-CPMAS NMR spectroscopy. ∥NMR was run on physically separated fractions only, not bulk soils. This data represents the clay size (<2 μm) fraction, which comprised 11–14% of soil mass. ¶Concentrations of compounds determined using a molecular mixing model[29]. #Concentrations of compounds determined by pyrolysis-GC/MS. **Mean and standard error of the free and bound total solvent-extractable lipids in mg g^{-1} C. ++Calculated as the ratio of n-C_{14} FA/(n-C_{14} FA + n-C_{26} FA); ref. 30). See Supplementary Table 2 for detailed lipid data. All values are means ± standard error unless noted otherwise.

be broken down. Differences in energy density in the Brady soil, defined as the total net exothermic energy content normalized by sample C content, also indicate differences in stability (Table 1).
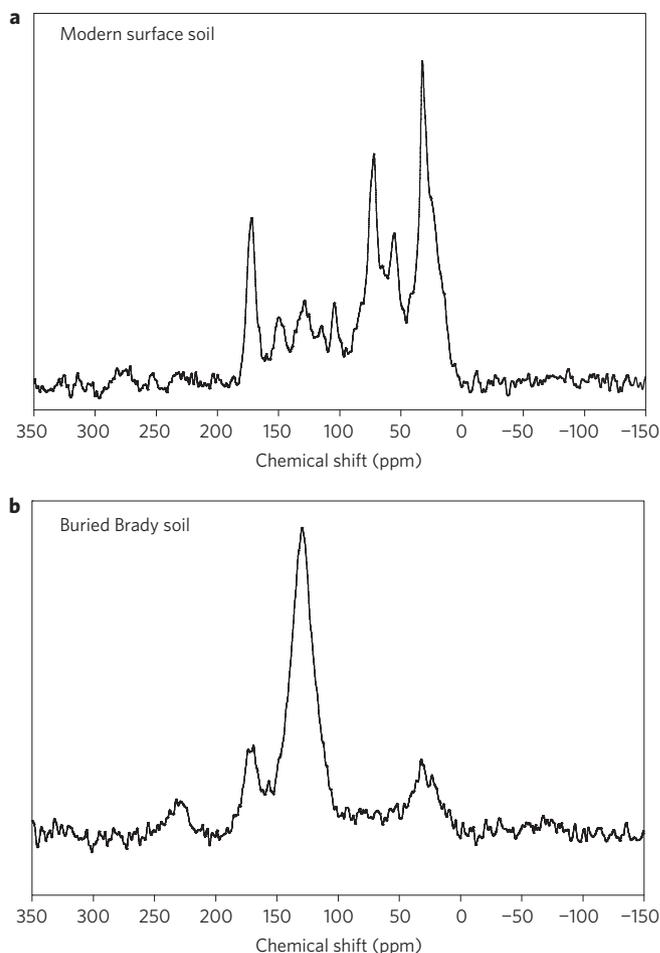
Within each soil layer, thermal analyses showed large compositional differences between fine (<20 μm) occluded particulate organic matter (oPOM-small) fractions, released from the disruption of soil
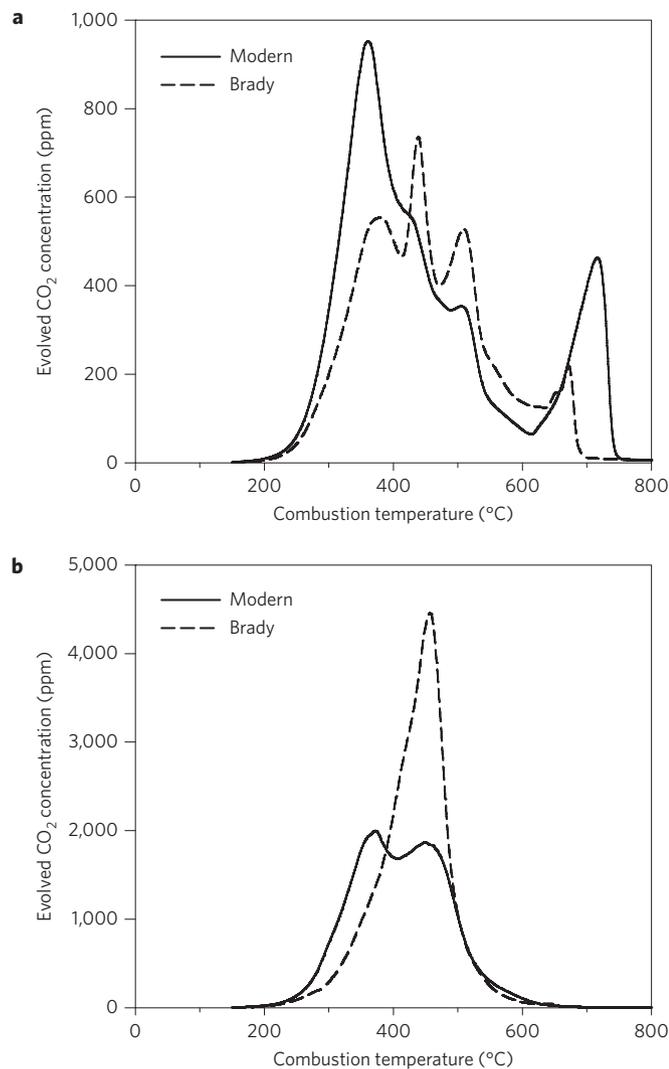
Figure 2 | Differences in thermal stability and evolution of CO₂ from modern and buried ancient soil organic matter from a loess sequence in southwestern Nebraska, USA. a,b, Evolved CO_2 during ramped combustion thermal analysis for bulk soil (**a**) and fine (<20 μm) occluded small particulate organic matter (oPOM-small) (**b**) samples from the modern surface soil (0–0.12 m) and buried Brady soil (6.35–6.50 m). The large peak in the bulk samples at >600 °C is generated by the presence of carbonates.

Figure 3 | Spectral differences in soil organic matter fractions between modern and buried soil show enrichment of pyrogenic C in the buried palaeosol. Solid-state CP MAS ¹³C-NMR spectra of the fine (<20 μm) occluded small particulate organic matter (oPOM-small) fractions isolated from the modern surface soil (0–0.12 m) (**a**) and buried Brady soil (6.35–6.50 m) (**b**). The chemical shift regions are representative of the following C functional groups: 0–45 ppm (alkyl C), 45–60 ppm (n-alkyl C), 60–95 ppm (O-alkyl C), 95–110 ppm (di-O-alkyl C), 110–145 ppm (aromatic C), 145–165 ppm (O-aryl C) and 165–185 ppm (carboxyl and carbonyl C). The peak at 130 ppm in the buried Brady soil is strongly indicative of pyrogenic or black C.

aggregates, and the bulk soil. As 90% of the bulk soil mass was recovered in the dense (>1.85 g ml⁻¹) fraction, this pool is expected to represent mineral-associated SOM. Comparison of the shapes of the evolved CO_2 thermograms (Fig. 2) were consistent with differences in the thermal stability between SOM associated with soil aggregates and that potentially sorbed to mineral surfaces. The greater thermal stability of the buried SOM relative to the modern surface soil, which suggests a more condensed aromatic structure, seems to be the result of pyrogenic alteration. Analyses by solid-state ¹³C-nuclear magnetic resonance (NMR) spectroscopy (Table 1) corroborated this observation. The oPOM-small fraction spectra were dominated by a large peak in the aromatic region at 130 ppm (Fig. 3), which is indicative of the presence of BC (ref. 15).

The enrichment of BC in the palaeosol compared to the modern soil indicates interactions between fire and erosion in the long-term sequestration of belowground C. The Brady SOM contained large proportions of BC, contributing up to 44% of the total signal intensity for the clay-sized mineral fraction and 72% for the oPOM-small fractions (Table 1 and Supplementary Table 1).

This accumulation of BC in the Brady soil could be explained by greater fuel loads and extensive fire during its exposure and pedogenesis. Regional palaeoclimatic studies suggest that the Brady soil experienced a period of recurring drought conditions before burial by increasing rates of dust aggradation[2,4]. The early Holocene in this region, during the time when the Brady soil was developing at the land surface, was characterized by a shift from C₃-dominated plant communities—cool season grasses, trees and shrubs—to communities dominated by C₄-warm season grasses, attributed to warmer temperatures[3,13,16]. The expansion of warm season grasses probably provided a positive feedback to fire. Continued warming and drier-than-present conditions[17] as the early Holocene progressed would have reduced vegetative cover and re-activated dune fields across the Great Plains region. The widespread deposition of loess downwind from proximal sources contributed to the burial of the Brady soil (Fig. 1; ref. 14).

The post-burial, selective preservation of BC under conditions unfavourable for decomposition also probably contributed to BC enrichment in the Brady soil. The preferential accumulation of BC

and plant biomarkers relative to other compounds in the occluded POM and in the dense, mineral-associated C fractions suggests physical protection as the primary mechanism for the long-term persistence of SOM in this environment. BC may play an active role in the formation and stabilization of soil aggregates[18] through hydrophobic interactions and as a hotspot of microbial activity. Variable rates of BC decay in the literature[7] support the premise that unfavourable conditions for microbial respiration, and not just chemical modifications by fire, contributed to the long-term persistence of BC in the buried palaeosol. Continued deposition of loess during formation of the Brady soil, although slow enough to allow for pedogenesis, would have buried BC progressively under thin layers of aggrading dust. Prolonged arid conditions during the accumulation of overlying loess and low mean annual precipitation today at the site also may have contributed to long-term persistence of buried Brady SOM.

Chemical data suggest that the stabilization of aged organic matter in the buried soil can be attributed to multiple mechanisms contributing to slowed decomposition. Decreasing concentrations of polysaccharides and lignin and an increase in aliphatic C in the Brady soil compared to the modern surface soil are consistent with expected greater alteration of plant-derived OM in aggregate-protected C fractions and in mineral soil layers with increased decay[19]. The Brady oPOM-small fractions contained greater n-C_{14} alkanoic acid concentrations, indicative of bacteria (Table 1), than did the modern soils. In contrast, the Brady soil had comparable concentrations of vascular plant-derived lipids (for example, triterpenoids, n-C_{25-31} alkanes, and n-C_{26-32} alkanoic acids) to those in the modern soil (Table 1). The persistence of plant lipids in the Brady soil for millennia suggests that environmental conditions in the buried soil have limited microbial transformation of organic matter.

The Brady SOM shows chemical characteristics typical of both deeper mineral horizons (>50 cm) in modern soils (low lignin, low carbohydrate content) and of modern surface soils (plant lipid persistence, BC enrichment), which can be interpreted in the context of its disturbance history. The stabilization of the Brady SOM occurred during a time of rapid regional warming and drying, probably driven by the Laurentide Ice Sheet retreat and increased summer insolation[4]. Rapid climatic changes triggered landscape disturbances[20] that created substantial deep soil OC reserves in the central US Great Plains. We estimate that the Brady soil, buried at various depths on stable uplands[2,13], could contain up to 2.7 Pg OC, assuming a continuous distribution throughout the area where it has been found (Fig. 1; ref. 21). Based on our estimates that about 40% of the Brady bulk SOM is derived from fire (Table 1), the amount of BC stored in the Brady soil is comparable to the BC estimate for boreal forest soils worldwide[22]. Even if the Brady soil existed only over a quarter of the area where the discrete occurrences have been identified, it would store up to 675.2 Mg OC—eight times that estimated to be buried under volcanic loess in 3 m-thick palaeosequences on the slopes of Mt. Kilimanjaro and 2.5 times that in surface soils of the Maasai steppe[10].

The accumulation of buried SOM in loess-palaeosol sequences provides evidence for the importance of feedbacks between climate and the land C sink at geologic and contemporary timescales[20,23]. Changes in landscape stability and sediment deposition rates driven by rapid shifts in climate and fire resulted in long-term stabilization of OC several metres below ground at depths below those accounted for in terrestrial C inventories and most biogeochemical models. Soil burial contributed to the persistence of vascular-plant lipids and fire-altered SOM in deep soil layers where conditions for microbial degradation are unfavourable. Recurring droughts during the Holocene have resulted in multiple aeolian depositional events[20], providing evidence for the sensitivity of landscape stability to changes in precipitation and land cover.

Future disturbances, for example, erosion and road construction that remove overlying sediments and alter hydrologic flowpaths, could reconnect buried soils to surface conditions and facilitate the mobilization and degradation of SOM (ref. 1), including BC (refs 15,24). Understanding the processes regulating deep soil C turnover can improve predictions of the potential for the release of ancient C to the atmosphere and of possible positive feedbacks to climate.

Methods

Site description, sampling and soil fractionation. This study was conducted in the loess-mantled uplands of southwestern Nebraska, USA (40° 29′ 59″ N, 101° 25′ 10″ W). Current vegetation at the site is shortgrass prairie grassland, mean annual temperature (MAT) is 9.7 °C, and mean annual precipitation (MAP) is 495 mm (climate data from High Plains Regional Climate Center, http://www.hprcc.unl.edu/data/historical/index.php). Soils were collected in triplicate, each sample about 5 m apart, from the modern (0–0.12 m depth) and Brady soil A horizons (6.35–6.5 m depth) at two replicate roadcuts (Old and New Wauneta Roadcuts) at 200 m distance from each other. The Brady soil A horizon has a silt loam texture and weak to moderate, fine or medium subangular blocky structure. Modern surface soils (A horizon) were sampled vertically from the surface terrain above the roadcuts and Brady soil samples were collected by cutting back from the face of the roadcuts to avoid eroded surface. The depth of the Brady soil had been pre-established from the landscape above the roadcuts using a Giddings coring device. All samples were air-dried and gently passed through a 2 mm sieve to remove coarse material—primarily roots. Using a combined density and particle size fractionation approach[25] with a low C–N sodium polytungstate solution ('SPT 0', $Na_6[H_2W_{12}O_{40}]$) (TC-Tungsten Compounds, Grub am Forst, Germany) at a density of 1.85 g cm^{-3}, we isolated three light density or particulate OM (POM) fractions—free, inter-aggregate POM (fPOM), small (<20 μm) and large (>20 μm) intra-aggregate or occluded POM (oPOM-small and oPOM-large)—and three heavy or mineral-associated OM particle size fractions—sand (>53 μm), silt (53–2 μm) and clay (<2 μm). Here we report chemical and isotopic data from the oPOM-small fractions, where the characteristic dark colour of the Brady soil was concentrated, and from bulk soils or clay-sized fractions. Estimated total soil organic C stored in the Brady soil regionally was calculated assuming a constant bulk density of 1.21 g cm^{-3}, 1 m thickness, and a spatial extent of 600 × 600 km (Fig. 1).

Elemental and isotopic analyses. Bulk soils and isolated physical fractions were analysed for total C and N concentrations and δ^{13}C at the UC Davis Stable Isotope Facility on an Elementar Vario EL Cube elemental analyser (Elementar Analysensysteme) connected to a PDZ Europa 20–20 isotope ratio mass spectrometer (Sercon Cheshire). All samples were run in duplicate, and duplicates were averaged. Samples for organic C concentrations and C isotopes were pre-treated by acid fumigation to remove carbonates[26]. Two replicate surface soil bulk samples and oPOM-small from the modern and Brady soil A horizons from the two replicate roadcuts were graphitized in the Houghton Carbon, Water and Soils Lab, USDA-FS Northern Research Station and analysed for ^{14}C on a Van de Graaff FN accelerator mass spectrometer (AMS) at the Center for AMS, Lawrence Livermore National Lab. Radiocarbon ages were calibrated with Calib v.6 using the IntCal09 dataset[27].

Thermal analyses. The thermal stability of SOM was used as a proxy for SOM biogeochemical stability, where greater biogeochemical stability is generally reflected by higher combustion temperatures at which 50% of sample mass is lost (TG–T_{50}) or 50% of evolved CO_2 is released (CO_2–T_{50}) during a ramped oxidation of samples. Bulk soil and oPOM-small samples of the modern surface and Brady soil horizons from the Old and New Wauneta Roadcuts were analysed at the University of Pennsylvania using a Netzsch STA409PC Luxx simultaneous thermal analyser for thermogravimetry (TG) and differential scanning calorimetry (DSC) coupled to a LICOR LI-840a IRGA for CO_2 and H_2O evolved gas analysis during the ramped combustion of samples at 10 °C min^{-1} up to 800 °C in a flowing CO_2-free artificial air atmosphere[28]. Energy density (in J mg^{-1} C) was determined as the area under the exothermic region of the DSC curve (150–615 °C) associated with OM combustion, normalized to the initial sample C concentration, and reflects the total bond energy, and thus the gross chemical composition, of the sample.

NMR analyses. Solid-state cross-polarization magic angle spinning ^{13}C nuclear magnetic resonance spectroscopy (CPMAS ^{13}C-NMR) was used to characterize the relative abundance of C functional groups of the modern surface and Brady soil fractions with a Bruker DSX 200 spectrometer (Bruker BioSpin) at the Lehrstuhl für Bodenkunde (TU München). Clay fractions were treated with HF

before NMR analysis to remove paramagnetic ions and to concentrate the C. Samples were filled into zirconium dioxide rotors and spun in a MAS probe at a rotation speed of 6.8 kHz to minimize chemical anisotropy. A ramped 1H pulse was used during a contact time of 1 ms to prevent Hartmann–Hahn mismatches. The delay time was set to 400 ms. Chemical shifts were referenced to tetramethylsilane (TMS = 0 ppm). NMR spectra were integrated within the following chemical shift (ppm) regions: 0–45 (alkyl C), 45–60 (n-alkyl C), 60–95 (O-alkyl C), 95–110 (di-O-alkyl C), 110–145 (aromatic C), 145–165 (O-aryl C) and 165–185 ppm (carboxyl and carbonyl C). The contributions of specific types of compounds (carbohydrates, proteins, lignin, lipids, and char) were estimated from the ^{13}C-NMR spectra by the application of a molecular mixing model that applies spectral information of known standards to calculate the proportion of specific compound types in unknown samples[29].

Lipid analyses. Duplicate modern surface bulk soils from the Old Wauneta Roadcut, Brady soil A horizon bulk soils from the Old and New Wauneta Roadcuts, one modern surface soil oPOM-small and two Brady oPOM-small fractions from the Old Roadcut and an additional Brady oPOM-small from the New Roadcut were quantitatively analysed for solvent-extractable lipid biomarkers at the University of Cincinnati. Samples were extracted on a Dionex ASE 350 accelerated solvent extractor with 2:1 dichloromethane/methanol (v/v). The extracts were base saponified at 70 °C in 0.5 M methanolic (3:1 methanol/water) KOH and then characterized and quantified on an Agilent 7890A/5975C GC-MSD/FID. Compounds were identified using authentic standards, published spectra, and retention times. Samples were normalized to grams of SOC. Precision and accuracy were determined with standards and were 4.5% and 2.6%, respectively.

Pyrolysis-GC/MS analyses. Pyrolysis gas chromatography mass spectrometry (Py/GC/MS) was used to identify classes of specific organic compounds in two replicate bulk soil samples and two oPOM-small fractions from the modern surface and Brady soil horizons at the University of New Hampshire on a CDS Pyroprobe 5150 pyrolyzer, Thermo Scientific Trace GC Ultra gas chromatograph and Thermo Scientific ITQ 900 mass spectrometer. Soils were pyrolyzed at 600 °C and transferred to a gas chromatograph with initial oven temperature increasing from 40 to 270 °C at a rate of 5 °C min^{-1} and a final rapid temperature ramp to 310 °C. Compounds were then transferred to the MS, where they were ionized at 200 °C. Peaks were identified using compound libraries developed using the National Institute of Standards and Technology (NIST) mass spectral library and published literature. Compound abundances were determined relative to the size of the largest compound peak within a sample.

References

1. Chaopricha, N. T. & Marin-Spiotta, E. Soil burial contributes to deep soil organic carbon storage. *Soil Biol. Biochem.* **69,** 251–264 (2014).
2. Mason, J. A., Jacobs, P. M., Hanson, P. R., Miao, X. & Goble, R. J. Sources and paleoclimatic significance of Holocene Bignell Loess, central Great Plains, USA. *Quat. Res.* **60,** 330–339 (2003).
3. Feggestad, A. J., Jacobs, P. M., Miao, X. & Mason, J. A. Stable carbon isotope record of Holocene environmental change in the central Great Plains. *Phys. Geogr.* **25,** 170–190 (2004).
4. Williams, J. W., Shuman, B., Bartlein, P. J., Diffenbaugh, N. S. & Webb III, T. Rapid, time-transgressive, and variable responses to early Holocene midcontinental drying in North America. *Geology* **38,** 135–138 (2010).
5. Rumpel, C. & Kögel-Knabner, I. Deep soil organic matter—a key but poorly understood component of terrestrial C cycle. *Plant Soil* **338,** 143–158 (2011).
6. Richter, D. D. & Mobley, M. L. Monitoring Earth's critical zone. *Science* **326,** 1067–1068 (2009).
7. Schmidt, M. W. I. *et al.* Persistence of soil organic matter as an ecosystem property. *Nature* **478,** 49–56 (2011).
8. Van Oost, K. *et al.* Legacy of human-induced C erosion and burial on soil-atmosphere C exchange. *Proc. Natl Acad. Sci. USA* **109,** 19492–19497 (2012).
9. Berhe, A. A. *et al.* Persistence of soil organic matter in eroding versus depositional landform positions. *J. Geophys. Res.* **117,** G02019 (2012).
10. Zech, M. *et al.* Buried black soils on the slopes of Mt. Kilimanjaro as a regional carbon storage hotspot. *Catena* **112,** 125–130 (2014).
11. Salomé, C., Nunan, N., Pouteau, V., Lerch, T. Z. & Chenu, C. Carbon dynamics in topsoil and in subsoil may be controlled by different regulatory mechanisms. *Glob. Change Biol.* **16,** 416–426 (2010).
12. Sankey, J. B., Germino, M. J. & Glenn, N. F. Aeolian sediment transport following wildfire in sagebrush steppe. *J. Arid Environ.* **73,** 912–919 (2009).
13. Johnson, W. C. & Willey, K. L. Isotopic and rock magnetic expression of environmental change at the Pleistocene–Holocene transition in the central Great Plains. *Quat. Int.* **67,** 89–106 (2000).
14. Mason, J. A. *et al.* Loess record of the Pleistocene–Holocene transition on the northern and central Great Plains, USA. *Quat. Sci. Rev.* **27,** 1772–1783 (2008).
15. Hockaday, W. C., Grannas, A. M., Kim, S. & Hatcher, P. G. The transformation and mobility of charcoal in a fire-impacted watershed. *Geochim. Cosmochim. Acta* **71,** 3432–3445 (2007).
16. Johnson, W. C., Willey, K. L. & Macpherson, G. L. Carbon isotope variation in modern soils of the tallgrass prairie: Analogues for the interpretation of isotopic records derived from paleosols. *Quat. Int.* **162–163,** 3–20 (2007).
17. Miao, x. *et al.* A 10,000 year record of dune activity, dust storms, and severe drought in the central Great Plains. *Geology* **35,** 119–122 (2007).
18. Brodowski, S., John, B., Flessa, H. & Amelung, W. Aggregate-occluded black carbon in soil. *Eur. J. Soil Sci.* **57,** 539–546 (2006).
19. Marschner, B. *et al.* How relevant is recalcitrance for the stabilization of organic matter in soils? *J. Plant Nutrition Soil Sci.* **171,** 91–110 (2008).
20. Arbogast, A. F. Stratigraphic evidence for late-Holocene aeolian sand mobilization and soil formation in south-central Kansas, USA. *J. Arid Environ.* **34,** 403–414 (1996).
21. Jacobs, P. M. & Mason, J. A. Impact of Holocene dust aggradation on A horizon characteristics and carbon storage in loess-derived Mollisols of the Great Plains, USA. *Geoderma* **125,** 95–106 (2005).
22. Ohlson, M., Dahlberg, B., Økland, T., Brown, K. J. & Halverson, R. The charcoal carbon pool in boreal forest soils. *Nature Geosci.* **2,** 692–695 (2009).
23. Zech, R. A permafrost glacial hypothesis - Permafrost carbon might help explaining the Pleistocene ice ages. *Quat. Sci. J.* **61,** 84–92 (2012).
24. Jaffé, R. *et al.* Global charcoal mobilization from soils via dissolution and riverine transport to the oceans. *Science* **340,** 345–347 (2013).
25. Mueller, C. W. & Kögel-Knabner, I. Soil organic carbon stocks, distribution, and composition affected by historic land use changes on adjacent sites. *Biol. Fertility of Soils* **45,** 347–359 (2008).
26. Harris, D., Horwarth, W. R. & Kessel, C. V. Acid fumigation of soils to remove carbonates prior to total organic carbon or carbon-13 isotopic analysis. *Soil Sci. Am. J.* **65,** 1853–1856 (2001).
27. Reimer, P. J. *et al.* IntCal09 and marine09 radiocarbon age calibration curves, 0–50,000 years cal BP. *Radiocarbon* **51,** 1111–1150 (2009).
28. Fernández, J. M., Peltre, C., Craine, J. M. & Plante, A. F. Improved characterization of soil organic matter by thermal analysis using CO_2/H_2O evolved gas analysis. *Environ. Sci. Technol.* **46,** 8921–8927 (2012).
29. Nelson, P. N. & Baldock, J. A. Estimating the molecular composition of a diverse range of natural organic materials from solid-state ^{13}C NMR and elemental analyses. *Biogeochemistry* **72,** 1–34 (2005).
30. Otto, A., Shunthirashingham, C. & Simpson, M. J. A comparison of plant and microbial biomarkers in grassland soils from the Prairie Ecozone of Canada. *Org. Geochem.* **36,** 425–448 (2005).

Author contributions

E.M-S., N.T.C. and J.A.M. conceived and designed the study; N.T.C. performed soil fractionation; A.F.P. performed thermal analyses; A.F.D. performed lipid analyses; C.W.M. performed NMR analyses; A.S.G. performed pyrolysis GC/MS analyses; E.M-S. wrote the manuscript; and all authors took part in the interpretation of the results.

Additional information

Supplementary information is available in the online version of the paper. Reprints and permissions information is available online at www.nature.com/reprints. Correspondence and requests for materials should be addressed to E.M-S.

Competing financial interests

The authors declare no competing financial interests.